Inorg. Chem. **2006**, *45*, 322–327

Synthesis of a One-Dimensional Metal-Dimer Assembled System with Interdimer Interaction, $M_2(dtp)_4$ (M = Ni, Pd; dtp = Dithiopropionato)

Atsushi Kobayashi,*,‡ Takahiko Kojima,‡ Ryuichi Ikeda,† and Hiroshi Kitagawa*,‡

Department of Chemistry, Faculty of Science, Kyushu University, Hakozaki 6-10-1, Higashi-ku, Fukuoka 812-8581, Japan, and Department of Chemistry, University of Tsukuba, Tennodai 1-1-1, Tsukuba, Ibaraki 305-8571, Japan

Received August 15, 2005

A metal-dimer assembled system, $M_2(dtp)_4$ (M = Ni, Pd; dtp = dithiopropionate, $C_2H_5CS_2^-$), was synthesized and analyzed by the X-ray single-crystal diffraction method, UV–vis–near-IR spectra of solutions, solid-state diffuse reflectance spectroscopies, and electrical conductivity measurements. The structures exhibit one-dimensional metal-dimer chains of $M_2(dtp)_4$ with moderate interdimer contact. These complexes are semiconducting or insulating, which is consistent with the fully filled d_{z^2} band of $M^{II}(d^8)$. Interdimer metal–metal distances were 3.644(2) Å in $Ni_2(dtp)_4$ and 3.428(2) Å in $Pd_2(dtp)_4$, each of which is marginally longer than twice the van der Waals radius of the metal. Interdimer charge-transfer transitions were nevertheless observed in diffuse reflectance spectra. The origin of this transition is considered to be due to an overlap of two adjacent d_{σ^*} orbitals, which spread out more than the d_{z^2} orbital because of the antibonding d_{σ^*} character of the $M(d_{z^2})$–$M(d_{z^2})$. The $Ni_2(dtp)_4$ exhibited an interdimer charge-transfer band at a relatively low energy region, which is derived from the Coulomb repulsion of the $3d_{\sigma^*}$ orbital of Ni.

Introduction

Since the discovery of metallic conductivity in the transition-metal complex tetracyanoplatinate, $K_2Pt(CN)_4X_{0.3}\cdot nH_2O$ (X = Cl, Br,)[1] commonly called KCP, a large number of KCP type (direct-chain type) complexes such as Magnus' green salt,[2] bis(oxalato)platinate,[3] and $Pt(bqd)_2$ (bqd = benzoquinonedioxime)[4] have been synthesized, and some of them exhibit metallic conductivity. As illustrated in Figure 1a, this type of complex consists of square-planar monomeric $[PtL_4]$ ions stacked along the direction perpendicular to the $[PtL_4]$ plane, forming a one-dimensional (1D) direct-chain structure. It is well-known that their metallic conduction properties arise from electron delocalization in a band formed by overlapped d_{z^2} orbitals. The overlapping of $5d_{z^2}$ orbitals strongly depends on the Pt−Pt distances, which vary widely from 3.71 Å in $Na_2[Pt(CN)_4]\cdot 3H_2O$[5] and 3.09 Å in

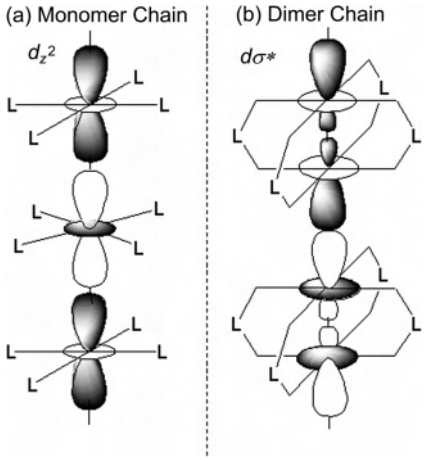

Figure 1. Schematic description of 1D chain structures with (a) monomeric and (b) dimeric units. Orbitals represent the HOMO of those units.

* To whom correspondence should be addressed. E-mail: akobascc@mbox.nc.kyushu-u.ac.jp (A.K.), hiroshiscc@mbox.nc.kyushu-u.ac.jp (H.K.).
‡ Kyushu University.
† University of Tsukuba.

(1) (a) Yersin, H.; Gliemann, G. *Ann. N.Y. Acad. Sci.* **1978**, *313*, 539. (b) Miller, J. S. *Extended Linear Chain Compounds*; Plenum Press: New York, 1982. (c) Miller, J. S.; Epstein, A. *Prog. Inorg. Chem.* **1976**, *20*, 1.
(2) (a) Magnus, G. *Ann. Phys. (Weinheim, Ger.)* **1828**, *14*, 239. (b) Martin, D. S., Jr.; Rush, M. R.; Kroening, R. F.; Fanwick, P. E. *Inorg. Chem.* **1973**, *12*, 301. (c) Atoji, M.; Richardson, J. W.; Rundle, R. E. *J. Am. Chem. Soc.* **1957**, *79*, 3017.
(3) (a) Krogmann, K. *Angew. Chem., Int. Ed.* **1969**, *8*, 35. (b) Kobayashi, H.; Shirotani, I.; Kobayashi, A.; Sasaki, Y. *Solid State Commun.* **1980**, *36*, 477.
(4) (a) Megnamisi, B. M. *J. Solid State Chem.* **1979**, *27*, 389. (b) Brill, J. W.; Megnamisi, B. M.; Novotny, M. *J. Chem. Phys.* **1978**, *68*, 585.
(5) Johnson, P. L.; Koch, T. R.; Williams, J. M. *Acta Crystallogr., Sect. B: Struct. Sci.* **1977**, *33*, 884.

10.1021/ic051387f CCC: $33.50
Published on Web 12/01/2005

$Sr[Pt(CN)_4]\cdot 3H_2O$[6] to 2.89 Å (slightly longer than the Pt−Pt distance of 2.77 Å in platinum metal) in the partially oxidized KCP(Br). Compared to the nickel or palladium 1D system, much more attention has been given to the direct-stacked Pt-chain system. One of the major reasons is the following. Pt has a larger d_{z^2} orbital than Ni or Pd, resulting in a large transfer integral for overlap of d_{z^2} orbitals along the 1D chain, leading to wider electronic bands and, consequently, a stabilized metallic state.

On the other hand, few examples of 1D direct-chain type systems composed of dimeric $[M_2L_4]$ units, as shown in Figure 1b, have been reported. In such a metal-dimer system, an internal degree of freedom of charge polarization is introduced into the $[M_2L_4]$ units, and therefore, a dynamic charge fluctuation of the metal can be expected. In fact, halogen-bridged 1D binuclear-metal mixed-valence complexes (the so-called MMX chain, which is not a direct-chain type) show a wide variety of electronic structures, and also exhibit many kinds of interesting physical properties, such as metallic conduction,[7] spin-Peierls transition,[7] and photo-induced phase transition.[8] In addition, a large number of nondirect-chain type complexes containing metal-dimer units and bridging organic molecules have been synthesized,[9,10] and they exhibit interesting phenomena involving magnetic properties coupled with charge transfer from metal dimers to organic molecules.[10]

In a 1D metal-dimer system, there are two important features. One is a decrease in electron repulsion. Compared with the monomer-chain type, the on-site Coulomb repulsion U is expected to be reduced because of the antibonding d_{σ^*} character of the $M(d_{z^2})-M(d_{z^2})$ direct overlap. This may contribute to high electrical conduction. The other is an extension of the limit of the interactive distance between adjacent units. Sakai et al. reported with regard to 1D platinum complexes that the limit of this interactive distance is longer in the dimer-chain type (ca. 3.9 Å) than in the monomer-chain type (ca. 3.3 Å).[11] These two features, which are mainly caused by an expanded d_{σ^*} molecular orbital formed by two d_{z^2} atomic orbitals, are expected to stabilize metallic conduction, that is, to increase the bandwidth W and reduce the on-site Coulomb repulsion U. Although the monomer-chain type Ni complex is expected to provide a unique opportunity for the construction of a strongly correlated 1D electron system, most of them are insulating because of a small overlapping of $3d_{z^2}$ atomic orbitals and a large U. In the Ni dimer-chain type, however, electron repulsion U and electron delocalization W would be reduced and increased, respectively, and compete with each other, resulting in novel physical properties and phenomena derived from a Mott−Hubbard 1D electron system ($U \sim W$).

Therefore, we report on a new direct-chain type metal-dimer system, $M_2(dtp)_4$ (M = Ni, Pd; dtp = $C_2H_5CS_2$), and discuss the electronic states of these complexes on the basis of their crystal structures and optical properties. Because these complexes have d^8-d^8 electronic configurations and a fully occupied d_{σ^*} band, the metallic conductivity could not be expected. However, if the partially filled d_{σ^*} band could be formed by electrical oxidation, these complexes would be attractive materials because of the competition between U and W.

Experimental Section

Syntheses. Dithiopropionic acid, Hdtp, was prepared according to the method previously reported.[12] Elemental analyses were performed by a Perkin-Elmer 2400 series II CHNS/O analyzer at the Chemical Analysis Center, University of Tsukuba.

$Ni_2(dtp)_4$ (1). $NiCl_2\cdot 6H_2O$ (1.19 g, 5 mmol) was dissolved in 30 mL of ethanol. To this light green solution was added a solution of Hdtp (1.62 g, 10 mmol) in 30 mL of diethyl ether. The solution color turned dark-violet immediately, and a purple precipitate emerged after 1 h. The suspension was kept stirring for 1 h at room temperature (rt), and was then kept in a refrigerator at 5 °C for 1 day. The crude product was collected by filtration, washed with ethanol, and recrystallized from CS_2 to afford 0.806 g (60% yield based on $NiCl_2\cdot 6H_2O$) of **1** as black needles with luster. Anal. Calcd for $C_{12}H_{20}Ni_2S_8$: C, 26.43; H, 3.75; S, 47.51. Found: C, 26.28; H, 3.91; S, 47.29.

$Pd_2(dtp)_4$ (2). To a solution of Hdtp (1.00 g, 9.42 mmol) in 45 mL of diethyl ether was added K_2PdCl_4 (1.02 g, 3.14 mmol, solid). The mixture was stirred for 2 days at rt. The light-orange solution slowly turned muddy dark-orange. The crude product was collected, washed with diethyl ether, and dissolved into CS_2. The solution was filtered, and the filtrate was kept at rt for slow evaporation of the solvent to afford 0.917 g (92% yield based on K_2PdCl_4) of **2** as black-yellow plate crystals with luster. Anal. Calcd for $C_{12}H_{20}Pd_2S_8$: C, 22.75: H, 3.18; S, 40.48. Found: C, 22.63; H, 3.22; S, 40.03.

$Pt_2(dtp)_4$ (3). Tetra-dithiopropionate-diplatinum, $Pt_2(dtp)_4$, was prepared according to the method previously reported,[13] and the purity was checked by elemental analysis and powder X-ray diffraction measurements.

(6) Krogmann, K.; Underhill, A. E. *Chem. Soc. Rev.* **1972**, *1*, 99.

(7) (a) Bellitto, C.; Flamini, A.; Gastaldi, L.; Scaramuzza, L. *Inorg. Chem.* **1983**, *22*, 444. (b) Kitagawa, H.; Onodera, N.; Sonoyama, T.; Yamamoto, M.; Fukawa, T.; Mitani, T.; Seto, M.; Maeda, Y. *J. Am. Chem. Soc.* **1999**, *121*, 10068. (c) Mitsumi, M.; Murase, T.; Kishida, H.; Yoshinari, T.; Ozawa, Y.; Toriumi, K.; Sonoyama, T.; Kitagawa, H.; Mitani, T. *J. Am. Chem. Soc.* **2001**, *123*, 11179. (d) Mitsumi, M.; Kitamura, K.; Morinaga, A.; Ozawa, Y.; Kobayashi, M.; Toriumi, K.; Iso, Y.; Kitagawa, H.; Mitani, T. *Angew. Chem., Int. Ed.* **2002**, *41*, 2767.

(8) (a) Matsuzaki, H.; Kishida, H.; Okamoto, H.; Takizawa, K.; Matsunaga, S.; Takaishi, S.; Miyasaka, H.; Sugiura, K.; Yamashita, M. *Angew. Chem., Int. Ed.* **2005**, *44*, 3240. (b) Kurmoo, M.; Clark, R. J. H. *Inorg. Chem.* **1985**, *24*, 4420. (c) Che, C.; Herbstein, F. H.; Schaefer, W. P.; Marsh, R. E.; Gray, H. B. *J. Am. Chem. Soc.* **1983**, *105*, 4604.

(9) (a) Cotton, F. A.; Dikarev, V. E.; Petrukhina, A. M.; Schmitz, M.; Stang, J. P. *Inorg. Chem.* **2002**, *41*, 2903. (b) Cotton, F. A.; Donahue, J. P.; Murillo, C. A. *Inorg. Chem. Commun.* **2002**, *5*, 59. (c) Sowa, T.; Kawamura, T.; Shida, T.; Yonezawa, T. *Inorg. Chem.* **1983**, *22*, 56. (d) Takizawa, Y.; Yang, Z.; Ebihara, M.; Inoue, K.; Kawamura, T. *Chem. Lett.* **2003**, *32*, 120. (e) Fuma, Y.; Ebihara, M.; Kutsumizu, S.; Kawamura, T. *J. Am. Chem. Soc.* **2004**, *126*, 12238.

(10) (a) Dunbar, K. R.; Powell, D.; Walton, R. A. *Inorg. Chem.* **1985**, *24*, 2842. (b) Dunbar, K. R.; Matonic, J. H.; Saharan, V. P. *Inorg. Chem.* **1994**, *33*, 25. (c) Miyasaka, H.; Campos-Fernandez, S. C.; Clerac, R.; Dunbar, K. R. *Angew. Chem., Int. Ed.* **2000**, *39*, 21. (d) Bera, J. K.; Vo, T.; Walton, R. A.; Dunbar, K. R. *Polyhedron* **2003**, *22*, 3009. (e) Cotton, F. A.; Lin, C.; Murillo, C. A. *J. Am. Chem. Soc.* **2001**, *123*, 2670. (f) Bartley, S. L.; Dunbar, K. R. *Angew. Chem., Int. Ed.* **1991**, *30*, 448.

(11) Takahashi, S. M.S. Thesis, Tokyo University of Science, Tokyo, 2002.

(12) Hartke, K.; Rettberg, N.; Dutta, D.; Gerber, H. D. *Liebigs Ann.* **1993**, 1081.

(13) Mitsumi, M.; Yoshinari, T.; Ozawa, Y.; Toriumi, K. *Mol. Cryst. Liq. Cryst.* **2000**, *342*, 127.

Table 1. Selected Crystallographic Data for **1** and **2**

	1	**2**
chemical formula	$C_6H_{10}S_4Ni$	$C_6H_{10}S_4Pd$
fw	269.09	316.79
T (K)	293	293
cryst syst	tetragonal	tetragonal
space group	$P4/n$ (No. 85)	$P4/n$ (No. 85)
a (Å)	12.9440(13)	13.0892(8)
c (Å)	6.1728(14)	6.1636(11)
V (Å)	1034.2(3)	1056.0(2)
Z	4	4
collected reflns	1332	1346
indep. reflns	1293	1307
no. of params	54	54
R^a	0.0342	0.0214
$R_w{}^b$	0.1334	0.0565
GOF	1.022	1.030

[a] $R = \sum||F_o| - |F_c||/\sum|F_o|$. [b] $R_w = [\sum w(|F_o| - |F_c|)^2/\sum wF_o^2]^{1/2}$, where w = least-squares weights.

UV−Vis−Near-IR Spectroscopy. UV−Vis−near-IR spectra of the complexes in toluene solution were recorded on a Jasco V-570 spectrophotometer.

Diffused Reflectance Spectroscopy. Diffuse reflectance spectra of the complexes diluted with KBr powder were recorded on a Jasco V-570 spectrophotometer equipped with a Jasco ISN-470 60 mmφ integrating-sphere apparatus. The obtained reflectance spectra were converted to absorption spectra using the Kubelka−Munk function $F(R_\infty)$.

Electrical Conductivity Measurements. The dc electrical conductivity measurements were performed along the chain axis (//c) between 250 and 300 K on a single crystal, using gold paint and gold wire (10 $\mu\phi$), by a conventional four-probe method with an excitation of 0.01 μA for $Pt_2(dtp)_4$ **3** and a two-probe method with an excitation of 5 V for $Ni_2(dtp)_4$ **1** and $Pd_2(dtp)_4$ **2**. The temperature was measured with a calibrated silicon diode sensor (LakeShore DT-470) placed near the sample.

X-ray Crystal Structure Analyses. A summary of the crystallographic data for $Ni_2(dtp)_4$ **1** and $Pd_2(dtp)_4$ **2** is given in Table 1. Each crystal was mounted on a glass fiber with epoxy resin. All measurements were made on a Rigaku AFC-7R diffractometer with graphite monochromated Mo Kα radiation ($\lambda = 0.71069$ Å) and a rotating anode generator. Cell constants and an orientation matrix for data collection, obtained from least-squares refinements using the setting angles of 25 carefully centered reflections in the range of $28.89° < 2\theta < 29.93°$ for **1** and $29.01° < 2\theta < 29.95°$ for **2**, each corresponded to the primitive tetragonal cell. On the basis of the systematic absences of $hk0$ for $h + k \pm 2n$, we determined the space group to be $P4/n$. The data were collected at 293 K using the $\omega-2\theta$ scan technique to the maximum 2θ value of 55.0°. The data were corrected for Lorentz and polarization effects. The structures were solved by direct methods (SIR92),[14] and were expanded using Fourier techniques (DIRDIF99).[15] The final cycle of full-matrix least-squares refinement (SHELEXL97)[16] on F^2 was based on 1191 and 1206 observed reflections for **1**and **2**, respectively, and 54 variable parameters; the refinement converged with unweighted and weighted agreement factors of $R = 0.0342$ and $R_w = 0.133$ for **1**,and $R = 0.0214$, and $R_w = 0.0565$ for **2**. The non-hydrogen atoms were refined anisotropically. The hydrogen atoms were refined isotropically. The maximum and minimum peaks on the final difference Fourier map corresponded to 0.38 and −0.44 e Å^3 near Ni(1) for **1** and to 0.50 and −0.25 e Å^3 near Pd(2) for **2**, respectively. All calculations were performed using the CrystalStructure crystallographic software package.[17]

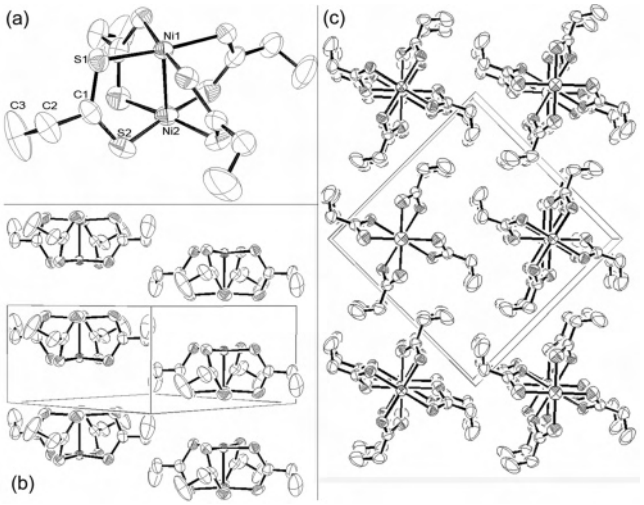

Figure 2. (a) Molecular structure, (b) 1D metal-dimer chain structure, and (c) packing diagram along the c axis (parallel to the dimer chain) of **1** with thermal vibrational ellipsoids at the 50% probability level. Hydrogen atoms are omitted for clarity.

Table 2. Selected Bond Distances (Å) and Angles (deg) for **1**[a]

Ni(1)−Ni(2)	2.5267(10)	Ni(1)−S(1)	2.2086(7)
Ni(2)−S(2)	2.2128(11)	S(1)−C(1)	1.677(3)
S(2)−C(1)	1.672(3)	C(1)−C(2)	1.519(5)
C(2)−C(3)	1.484(8)	Ni(1)···Ni(2)′	3.646(1)
Ni(1)−Ni(2)−S(2)	92.96(3)	S(1)−Ni(1)−Ni(2)	93.13(2)
Ni(1)−S(1)−C(1)	108.11(12)	Ni(2)−S(2)−C(1)	107.72(12)
C(1)−C(2)−C(3)	113.1(4)	S(1)−C(1)−S(2)	126.0(2)
S(1)−C(1)−C(2)	116.8(2)	S(2)−C(1)−C(2)	117.2(2)
Ni(2)−Ni(1)···Ni(2)′	180.00		

[a] A superscript prime refers to the following equivalent positions relative to the x, y, z set: $+x, +y, +1 + z$.

Results and Discussion

Crystal Structure of $Ni_2(dtp)_4$ (1) and $Pd_2(dtp)_4$ (2). The molecular structure of **1** is shown in Figure 2a. The palladium complex **2** had almost the same structure as that of **1**. Selected bond lengths (Å) and angles (deg) are summarized in Table 2 for **1** and Table 3 for **2**. The complexes **1** and **2** crystallized in tetragonal space group $P4/n$. Two metal atoms were bridged by four dtp ligands. Each metal atom had five neighbors, i.e., four sulfur atoms and a metal atom, in a tetragonally distorted square-pyramidal geometry. The M−M bond distances in the dimer unit were 2.5267(10) Å for **1** and 2.7247(5) Å for **2**. These M−M bond distances are almost equal to those in the metals (Ni, 2.50 Å; Pd, 2.76 Å). Despite the fact that the formal bond order of the M−M bond is zero, these M−M distances are surprisingly short, showing that there is a strong interaction between metal centers in a dimer unit. This structure is almost the same as

(14) Altomare, A.; Cascarano, G.; Giacovazzo, C.; Guagliardi, A.; Burla, M.; Polidori, G.; Camalli, M. SIR92. *J. Appl. Crystallogr.* **1994**, *27*, 435.

(15) Beurskens, P. T.; Admiraal, G.; Beurskens, G.; Bosman, W. P.; de Gelder, R.; Israel, R.; Smits, J. M. M. *DIRDIF99*; Crystallography Laboratory at University of Nijmegen: Nijmegen, The Netherlands, 1999.

(16) Sheldrick, G. M. *SHELX97*; University of Göttingen: Göttingen, Germany, 1997.

(17) *CrystalStructure 3.7.0: Crystal Structure Analysis Package*; Rigaku and Rigaku/MSC: Tokyo, 2000−2005.

Table 3. Selected Bond Distances (Å) and Angles (deg) for **2**[a]

Pd(1)−Pd(2)	2.7247(5)	Pd(1)−S(1)	2.3252(7)
Pd(2)−S(2)	2.3257(9)	S(1)−C(1)	1.675(3)
S(2)−C(1)	1.675(3)	C(1)−C(2)	1.518(4)
C(2)−C(3)	1.497(6)	Pd(1)···Pd(2)′	3.4387(5)
Pd(1)−Pd(2)−S(2)	91.12(2)	S(1)−Pd(1)−Pd(2)	91.16(2)
Pd(1)−S(1)−C(1)	109.43(11)	Pd(2)−S(2)−C(1)	108.86(11)
S(1)−C(1)−S(2)	128.66(19)	S(1)−C(1)−C(2)	115.3(2)
S(2)−C(1)−C(2)	116.0(2)	C(1)−C(2)−C(3)	112.1(3)
Pd(2)−Pd(1)···Pd(2)′	180.00		

[a] A superscript prime refers to the following equivalent positions relative to the *x*, *y*, *z* set: $+x$, $+y$, $+1 + z$.

that of the Pt complex Pt_2dtp_4 (**3**),[13] and the $M_2(dtp)_4$ (M = Ni, Pd, Pt) complexes are isomorphous to each other (the same space group of $P4/n$). Each of the $M_2(dtp)_4$ complexes shows an inward displacement from the S_4 plane to the direction of the other metal ion. This inward displacement from the S_4 plane is 0.12 Å in **1**, 0.04 Å in **2**, and 0.10 Å[13] in **3**,. These inward displacements from the S_4 plane also indicate the strong metal−metal interaction within the dimer. Other bond distances and angles are similar to the those values observed for analogues such as tetrakis(dithioacetato)-dimetal (metal = Ni, Pd, Pt),[18] bis(dithiobenzoate)metal (metal = Ni, Pd),[19] and tetrakis(phenyldithioacetato)-dinickel.[20] Tetrakis(phenyldithioacetato)dinickel has almost the same 1D dimer-chain structure as that of $M_2(dtp)_4$.

As shown in Figure 2b, metal-dimer units are stacked and form 1D metal-dimer chains. The interdimer M···M distances are 3.644(2) Å in **1**, 3.428(2) Å in **2**, and 3.428(1) Å in **3**. The Pt complex **3** has an interdimer M···M distance shorter than twice the van der Waals radius of the metal (Ni, 3.26 Å; Pd, 3.26 Å; Pt, 3.50 Å),[21] but the interdimer M···M distances of **1** and **2** are marginally longer than twice the van der Waals radius. In general, these rather long M···M distances imply that there are no or very weak interactions between adjacent metal-dimer units in the chains. However, for both **1** and **2**, we observed an interdimer charge-transfer absorption in the low-energy region (see later in paper).

The interdimer S···S distances in the 1D chains are 3.5937(13) Å in **1** and 3.5188(18) Å in **2**,, and these distances are slightly shorter than twice the van der Waals radius of the sulfur atom (3.60 Å).[21] This S···S contact may play a part in forming the 1D metal-dimer chain structures. On the other hand, interchain S···S distances are much longer, ca. 4.8 Å, indicating no S···S van der Waals interaction between the 1D chains. Judging from the crystal structure, complexes **1** and **2** are regarded as quasi-one-dimensional electronic systems.

Absorption Spectra. The UV−vis−near-IR spectra in toluene solutions of **1**, **2**, and **3** are shown in Figure 3. The

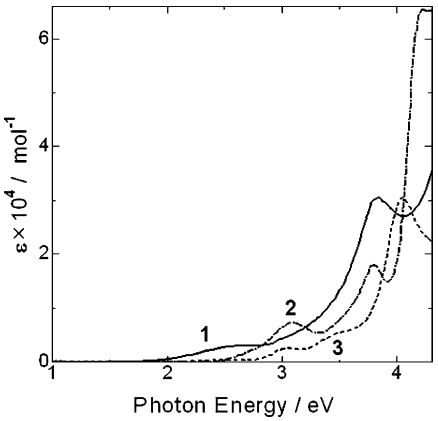

Figure 3. UV−vis−near-IR absorption spectra of $M_2(dtp)_4$. The spectra are plotted by a solid line for **1**, a one-point chain line for **2**, and a dashed line for **3**.

Table 4. Assignment of Observed Bands (eV) in UV−Vis−Near-IR Spectra of $M_2(dtp)_4$ in Toluene Solution

complex			
1	**2**	**3**	assignment
2.50	3.10	3.00 3.48	$d_{\sigma^*}(^1A_{1g}) \rightarrow p_\sigma(^3A_{2u})$
3.80	3.84 4.23	4.05	$d_{\sigma^*}(^1A_{1g}) \rightarrow p_\sigma(^1A_{2u})$ $d_{\pi^*} \rightarrow p_\sigma$

Table 5. Assignment of Observed Bands (eV) in Diffuse Reflectance Spectra of $M_2(dtp)_4$

complex			
1	**2**	**3**	assignment
1.70 2.20	2.00	2.00	IDCT
2.78 3.36	2.81 3.20	*2.88*	$d_{\sigma^*} \rightarrow p_\sigma$
3.75	3.56	3.70	$d_{\pi^*} \rightarrow p_\sigma$

assignments of observed bands are summarized in Table 4. In general, an intermolecular charge-transfer transition cannot be expected in dilute solution where the intermolecular interactions are negligible. A weak absorption peak was observed for each $M_2(dtp)_4$ complex, centered at 2.50 eV (496 nm) for **1** (ϵ = 2900), 3.10 eV (400 nm) for **2** (ϵ = 7500), and 3.00 eV (413 nm) for **3** (ϵ = 2600). As each of the $M_2(dtp)_4$ complexes has a d^8-d^8 electronic configuration with square-pyramidal geometry and a strong M−M bond, the HOMO (highest occupied molecular orbital) is thought to be d_{σ^*} [$d_{\sigma^*} = (d_{z^2}-d_{z^2})^*$]. Considering the relatively low ϵ, this weak absorption peak is assigned to the $d_{\sigma^*}(^1A_{2g}) \rightarrow p_\sigma(^3A_{2u})$ transition. Because this transition is formally spin-forbidden, the absorbance of this transition would be relatively low. A similar absorption peak was observed for $K_4[Pt_2(pop)_4]\cdot 2H_2O$ (pop = diphosphite), which is isoelectronic with **3**.[22] In the higher-energy region above 3.5 eV, very intense peaks were observed for each complex. These absorption peaks have been discussed for complexes with similar dimeric structures, such as $Pt_2(n\text{-}C_6H_{13}CS_2)_4$[23] and $K_4[Pt_2(pop)_4]\cdot 2H_2O$,[22,8b] and are suggested to correspond to $d_{\sigma^*}(^1A_{2g}) \rightarrow p_\sigma(^1A_{2u})$ and $d_{\sigma^*} \rightarrow p_\sigma$ transitions.

(18) (a) Furlani, C.; Flamini, A.; Piovesana, O.; Bellitto, C.; Sgamellotti, A. *J. Chem. Soc., Dalton Trans.* **1973**, 2404. (b) Piovesana, O.; Bellitto, C.; Flamini, A.; Zanazzi, P. F. *Inorg. Chem.* **1979**, *18*, 2258.
(19) (a) Furlani, C.; Luciani, M. L. *Inorg. Chem.* **1968**, *7*, 1586. (b) Bonamico, M.; Dessy, G.; Fares, V.; Scaramuzza, L. *J. Chem. Soc., Dalton Trans.* **1975**, 2250.
(20) (a) Bonamico, M.; Dessy, G.; Fares, V. *Chem. Commun.* **1969**, 1106. (b) Bonamico, M.; Dessy, G.; Fares, V. *J. Chem. Soc., Dalton Trans.* **1977**, 2315.
(21) Bondi, A. *J. Phys. Chem.* **1964**, *68*, 441.
(22) Che, M. C.; Schaefer, P. W.; Gray, B. H.; Dickson, K. M.; Stein, B. P.; Roundhill, D. M. *J. Am. Chem. Soc.* **1982**, *104*, 4253.
(23) Kawamura, T.; Ogawa, T.; Yamabe, T.; Masuda, H.; Taga, T. *Inorg. Chem.* **1987**, *26*, 3547.

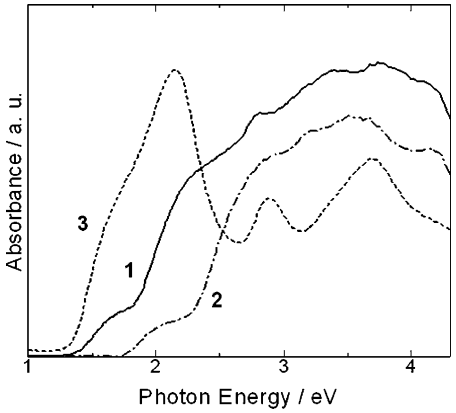

Figure 4. Diffuse reflectance spectra of $M_2(dtp)_4$. The spectra are plotted by a solid line for **1**, a one-point chain line for **2**, and a dashed line for **3**.

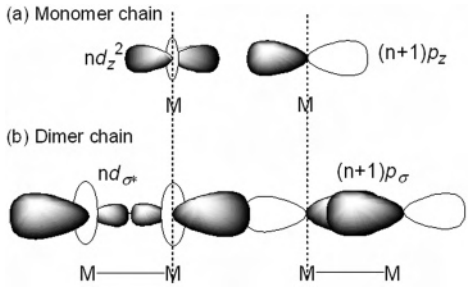

Figure 5. Schematic diagram of two metal units located in the same M···M distance that slightly exceeds twice the van der Waals radius of the metal. (a) In the case of a monomer chain. (b) In the case of a dimer chain.

Diffuse Reflectance Spectra. The diffuse reflectance spectra of **1**, **2**, and **3** are shown in Figure 4. The assignments of observed bands are summarized in Table 5. All $M_2(dtp)_4$ complexes exhibited absorption peaks below 2 eV. An especially intense absorption band was observed for **3**. No absorption peaks were observed in solutions in this region. This absorption band has been discussed and assigned to an interdimer charge-transfer (IDCT) transition[13,22] that arises from overlapping an nd_{σ^*} orbital with an $(n + 1)p_\sigma$ orbital of a neighboring dimer unit. Pt atoms with large $5d_{z^2}$ orbitals are capable of interacting with orbitals of neighboring atoms. Similar but weak shoulder peaks were observed at 1.7 eV for **1** and at 2.0 eV for **2**. As mentioned above, interdimer M···M distances in **1** and **2** are longer than twice the van der Waals radius of the corresponding metal, suggesting generally that there would be no direct interaction between adjacent dimers. However, taking into account the molecular orbital d_{σ^*} that is largely expanded outward, these weak peaks could be also assigned to IDCT. Namely, this large molecular orbital d_{σ^*} enables the metal dimers to interact with each other at distances beyond twice the van der Waals radius of the metal. Figure 5a shows a schematic diagram of two units (one indicates the HOMO (nd_{z^2}) and the other indicates the LUMO ($(n + 1)p_z$)) located at a certain distance that slightly exceeds twice the van der Waals radius of the metal, where there are no orbitals overlapping in the monomer chain and a CT band could not be observed. On the other hand, in the dimer chain, as shown in Figure 5b, because each unit has largely expanded occupied d_{σ^*} and unoccupied $(n + 1)p_\sigma$ orbitals, they overlap beyond twice the van der Waals radius and, consequently, the IDCT band can be observed. As mentioned in the Introduction, a dimer unit would bring about an increase in the maximum distance at which units can interact with each other. Sakai et al. reported about Pt complexes that there is certain interaction between Pt dimers with a distance of ca. 3.9 Å.[11] As mentioned so far, the observation of an IDCT band in **1** and **2** strongly indicates that the interactive distance in the dimer chain becomes longer than it is in the monomer chain.

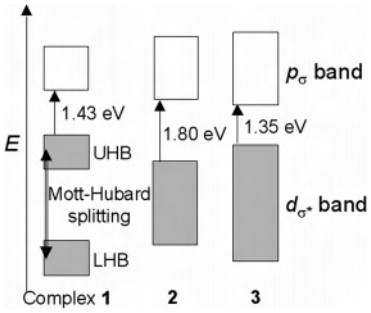

Figure 6. Schematic energy-band structure of the three $M_2(dtp)_4$ complexes. Energies represent the IDCT band edge.

Table 6. Electrical Conductivity at 300 K (σ_{300K}) and Activation Energy (E_a) of $M_2(dtp)_4$

complex	σ_{300K} (S cm^{-1})	E_a (eV)
1	7.0×10^{-9}	0.482
2	8.1×10^{-8}	0.448
3	4.5×10^{-3}	0.148

The lower-energy edge of IDCT bands shifts to the lower-energy side in the order of 1.80 eV in **2** > 1.43 eV in **1** > 1.35 eV in **3**, as expected for the larger d orbitals on going down the 3d−4d−5d series. These energies correspond to the energy gaps between HOMO (d_{σ^*}) and LUMO (p_σ) bands. Considering the size of the metal and the interdimer M···M distance, the band gap energy would be expected to be **1** > **2** > **3**. However, a consideration of electron correlation derived from the small 3d orbital of Ni must account for the reverse order of **1** and **2**. Namely, the Mott−Hubbard splitting[24] gives an explanation about this reverse order between **1** and **2**. The schematic energy diagram of $M_2(dtp)_4$ is shown in Figure 6. In Ni complex **1**, because of the strong electronic repulsion of the 3d orbital, the d_{σ^*} band is split into two bands, i.e., upper Hubbard band (UHB) and lower Hubbard band (LHB). The Mott−Hubbard splitting in **1** is so large that the energy gap between the UHB and the p_σ band becomes smaller than the gap in **2**.

Electrical Conductivity. The electrical conductivity at 300 K (σ_{300K}) and activation energy (E_a) for $M_2(dtp)_4$ (M = Ni, Pd, Pt) are summarized in Table 6. Each complex was semiconducting or insulating, but the conductivity of **3** was several orders of magnitude larger than that of **1** or **2**. The insulating or semiconducting property is consistent with the expected band structure composed from fully occupied d_{σ^*} and unoccupied p_σ bands, as shown in Figure 6. In general, the optical gap energy E_{opt} is larger than the band gap energy

(24) (a) Mott, N. F. *Metal−Insulator Transitions*; Taylor and Francis: London, 1974. (b) Austin, I. G.; Mott, N. F. *Science* **1970**, *168*, 71. (c) Zylbersztejn, A.; Mott, N. F. *Phys. Rev. B* **1975**, *11*, 4383.

E_g (=$2E_a$), which is measured as a thermal activation energy of conduction. According to the Franck−Condon principle, an optical transition of the electron occurs vertically between the potential energy curves, whereas the thermally activated hopping occurs through the crossing point of curves. When the curves are the $y = x^2$ forms of a parabola, $E_{opt} = 4E_a$, which is observed in some small-polaron solids. Each of the optical gaps observed for $M_2(dtp)_4$ is more than $2E_a$ and less than $4E_a$. The Pt complex **3** has the highest conductivity and smallest activation energy in $M_2(dtp)_4$, which is consistent with the smallest optical band gap observed in the diffuse reflectance spectra. Compared to the E_{opt}, this complex exhibited a much smaller E_a, which may be derived from the existence of impurity levels in the band gap.

Conclusion

We have synthesized and investigated a novel 1D metal-dimer assembled system $M_2(dtp)_4$. This system has short M−M distances and strong M−M interactions. They are semiconducting or insulating, which is consistent with the fully occupied d_{z^2} band. Although the interdimer M···M distance in the 1D chain of $M_2(dtp)_4$ is longer than twice the van der Waals radius of the metal, it exhibits an interdimer charge-transfer band in the low-energy region of 1.4−2.3 eV. The origin of the band is considered to be an overlapping of largely expanded nd_{σ^*} and $(n + 1)p_\sigma$ orbitals between adjacent metal dimers. Because of the strong electronic repulsion on the 3d orbital in $Ni_2(dtp)_4$, Mott−Hubbard splitting occurs in $3d_{\sigma^*}$ effectively, so that the optical band gap becomes smaller than that in $Pd_2(dtp)_4$. The $M_2(dtp)_4$ can be regarded as a new 1D electronic system composed of widely expanded d_{σ^*} and p_σ orbitals. Partial oxidation of these chains is in progress.

Acknowledgment. This work was partly supported by a Grant-in-Aid for Scientific Research (16074212) of Priority Areas (Chemistry of Coordination Space) and the Joint Project for Chemical Synthesis Core Research Institutions from the Ministry of Education, Culture, Sports, Science and Technology, Japan, by Grants-in-Aid for Scientific Research (B) (14340215 and 16350033) from the Japan Society for the Promotion of Science, and by the Kurata Memorial Hitachi Science and Technology Foundation and Grant for Basic Science Research Projects, the Sumitomo Foundation.

Supporting Information Available: X-ray crystallographic files in CIF format of **1** and **2**. This material is available free of charge via the Internet at http://pubs.acs.org.

IC051387F